Semiconductor Science and Technology

PAPER

Structural, optical and magnetic properties of a dilute magnetic semiconductor based on Ga-doped ZnO and Co

To cite this article: A Sh Asvarov *et al* 2020 *Semicond. Sci. Technol.* **35** 105003

IOP Publishing Semiconductor Science and Technology
Semicond. Sci. Technol. **35** (2020) 105003 (6pp) https://doi.org/10.1088/1361-6641/aba41b

Structural, optical and magnetic properties of a dilute magnetic semiconductor based on Ga-doped ZnO and Co

A Sh Asvarov[1,2,5], A V Butashin[1], V M Kanevsky[1], A E Muslimov[1], N S Perov[3] and A Chiolerio[4]

[1] Shubnikov Institute of Crystallography, Federal Scientific Research Center 'Crystallography and Photonics' of Russian Academy of Sciences, Moscow, Russia
[2] Institute of Physics, Dagestan Federal Research Center of Russian Academy of Sciences, Makhachkala, Russia
[3] Faculty of Physics, Lomonosov Moscow State University, Moscow, Russia
[4] Istituto Italiano di Tecnologia, Center for Sustainable Future Technologies, 10144, Torino, Italy

E-mail: abil-as@list.ru

Received 20 May 2020, revised 23 June 2020
Accepted for publication 8 July 2020
Published 21 August 2020

Abstract

A wide bandgap oxide/transition metal multilayered structure, consisting of four submicron-thick Ga-doped ZnO layers and three ultrathin Co metal layers, is studied to highlight the induction of room temperature ferromagnetism (RTFM), a fundamental outcome of investigations dealing with dilute magnetic semiconductors and multiferroic materials. A comprehensive study including the structural, optical and magnetic properties of both as-deposited and high-temperature annealed samples is described. Optical transmittance spectroscopy and x-ray diffraction measurements confirm the conversion of the layered structure into a solid-state solution of Co within the Ga-doped ZnO after annealing. The study discloses RTFM in the as-deposited state due to nonoxidized metal components within the multilayer structure.

Keywords: ZnO, diluted magnetic semiconductors, doping, multilayer, structure, annealing

(Some figures may appear in color only in the online journal)

1. Introduction

Materials based on systems containing abundant and non-toxic ZnO semiconductor and Co transition metal (TM) appear to have huge potential in various fields, such as transparent electrodes [1], anodes of Li-ion batteries [2], nonlinear optical elements [3, 4], piezoelectric and ferroelectric devices [5, 6], optical and gas sensors [7, 8] and catalysis [9, 10]. Additional great interest in the ZnO–Co system is triggered by its prospects for spin-based information processing technologies (spintronic applications) due to the discovery of room temperature ferromagnetism (RTFM) and multiferroic behaviors in this material [11–13].

Zinc oxide layers with controlled cobalt content in metal or oxide form have been deposited by several techniques including pulsed laser deposition [14, 15], the sol-gel method [10], molecular beam epitaxy [13], spray pyrolysis [1, 16], magnetron sputtering [17] and chemical vapor deposition [18]. Particularly, magnetron sputtering allows easy adaptation to the tasks of metal-doped ZnO [19–21] and binary oxides (for example, $ZnCo_2O_4$) [22], as well as obtaining multilayered structures [23, 24] on a variety of substrates. A ZnO/Co multilayer structure is particularly interesting in terms of precisely

[5] Author to whom any correspondence should be addressed.

controlling the amount of dopant as well as its depth profile by tuning the Co and ZnO sub-layer thicknesses and by performing a diffusive heat treatment after deposition [25].

Despite the fact that there are several reports on the magnetic properties of ZnO-based materials (frequently called diluted magnetic semiconductors—DMS), the origin of RTFM in TM-doped ZnO remains controversial. There is an ongoing debate on whether these materials have a really inherent ferromagnetism due to spin–orbit coupling between localized d-spins of magnetic dopants and delocalized electrons (intrinsic defect structure with magnetic order) or whether the observed magnetic behavior is due to nanometer-sized precipitates of the magnetic TM dopant atoms embedded in the nonmagnetic ZnO matrix [26, 27]. The detected oxidative quenching of RTFM in Co-doped ZnO DMS films due to the reduction of density of n-type defects, like oxygen vacancies [28], justifies studies related to ZnO-based DMS that are additionally doped with a metal belonging to group III (Al or Ga) in order to increase the concentration of charge carriers [14, 29, 30]. These materials hold great potential for manipulating magnetic exchange coupling strength. Ga-doped ZnO (GZO) has also been studied as a mixed oxide conductive transparent material for commercial applications [31].

In the present work, a GZO/Co multilayer structure was prepared using the magnetron sputtering method. The structural, morphological, optical and magnetic properties were studied. The transformation of the properties of such a multilayer structure after diffusive high-temperature annealing was studied.

2. Experimental

A Ga-doped ZnO/Co multilayer sample was grown by magnetron sputtering of ceramic GZO and metallic Co (with a purity of 99.95%) targets 75 mm in diameter on quartz substrate at 4 × 4 cm^2 at a substrate temperature of 250 °C. The GZO ceramic target with a Ga doping level of 3% mol. was sintered at 1400 °C for 10 h by a solid-state reaction. The base pressure before sputtering was kept below 5×10^{-5} Pa and the sputtering was performed in an Ar atmosphere at a pressure of 0.5 Pa. A GZO/Co multilayer structure with seven layers was fabricated by alternate positioning of the substrate in front of the corresponding magnetron unit. The distance between the targets and the substrate was kept fixed at 10 cm during the film deposition. The GZO and Co targets were sputtered in radio-frequency mode with a power $P_{RF} = 110$ W and at higher wavelengths with $P_{MF} = 65$ W (frequency $\nu_{MF} = 15$ kHz, duty cycle D_{MF} of 50%), respectively. The multilayer growth scheme is depicted in figure 1(a). The deposition time of each even oxide layer was 10 min, while the odd Co layers were deposited for 1 min. Some as-deposited samples were annealed at 800°C for 60 min in air. Hereafter, the as-deposited and annealed samples will be named S0 and S1, respectively.

X-ray diffraction (XRD) measurements were carried out on a X'Pert Pro MPD diffractometer (PANalytical) with a CuKα source. The surface morphology and chemical composition

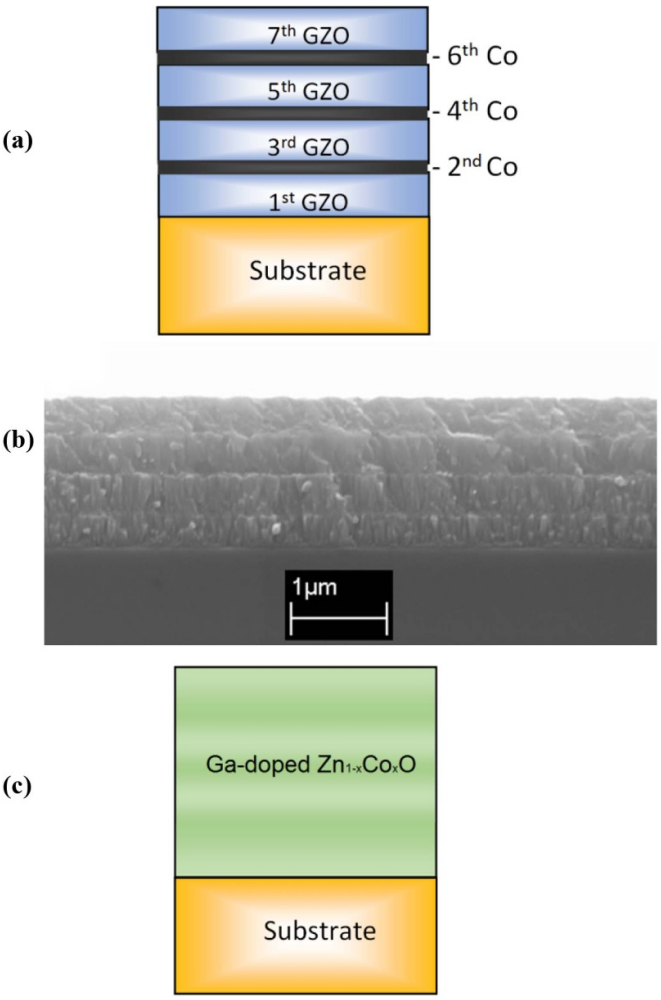

Figure 1. Scheme of as-prepared multilayer structure (a), SEM image of as-prepared multilayer structure (b) and scheme of structure after air annealing (c).

were investigated using the scanning electron microscope (SEM) Leo-1450 equipped with an energy dispersive x-ray (EDX) spectrometer (Inca-200, Oxford Instruments). The optical transmission properties were tested using a UV–Vis–NIR double-beam spectrophotometer (Shimadzu UV-3600). The magnetic properties of the samples were measured using a vibrating sample magnetometer (VSM LakeShore 7407 model) with an applied field of ±15 kOe at room temperature. The contribution of the sample holder rod was taken into account by preliminarily measuring the field dependences for the empty rod and subtracting these data from the subsequent measurement results for the sample glued to the rod.

3. Results and discussions

Figure 1(b) shows a cross-sectional SEM image collected from the sample S0, prepared by simple cleavage of the substrate with the as-deposited seven-layer structure on it. It can be seen that the introduction of the three ~15 nm thick Co interlayers into the multilayered structure results in breaking the GZO layer into four equal parts whose thickness is around 360 nm.

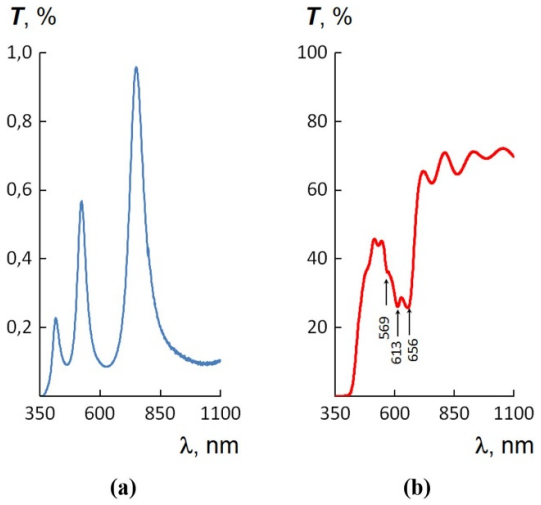

Figure 2. Optical transmittance spectra of the as-prepared (a) and annealed (b) samples.

The total thickness of the multilayer is around 1500 nm. The oxide components of the S0 multilayer structure are columnar in nature, which is a characteristic feature of ZnO thin films.

The presence of metal interlayers in the S0 structure gives it a 'mirror' appearance in the visible and near-infrared regions. Due to the high reflection coefficient, only a small part of the incident electromagnetic radiation passes through the multilayer structure S0 (figure 2(a)). According to figure 2(a), the optical transmission of S0 is less than 1% in the measured wavelength range. The observed interference fringes in the spectrum are due to repeated reflections of light passing into the oxide layers at their interfaces. Such a beating-free oscillatory nature in the spectrum indicates a high repeatability of the growth process for all the GZO oxide layers of the S0 multilayer in both thickness and structure. It can be noticed that adjusting the optical properties of multilayer structures by a certain optimization of the thicknesses of oxide and metal interlayers makes it possible to use such structures for anti-laser striking (optical filters) and laser-induced THz radiation source applications [32, 33].

The as-deposited samples were annealed at 800 °C in air for 1 h. The transmittance value was found to increase significantly after air annealing (figure 2(b)) and the color of the annealed sample turned green. This green color is correlated with the typical d–d transition of high spin states of Co^{2+} in tetrahedral oxygen coordination. In the transmittance spectrum of the S1 sample there are three deep absorption edges at around 569 nm, 613 nm and 656 nm. The observation of these characteristic absorption bands indicates that the Zn^{2+} ions are replaced by Co^{2+} ions in the wurtzite crystal structure of ZnO without destroying its order. Furthermore, from comparing the two spectra, it can be seen that the periodicity of interference fringes of sample S1 increases with respect to sample S0. This fact, along with an increase in transparency, and the appearance of significant absorption bands, indicates that the air annealing leads to diffuse dissolution and oxidation of thin cobalt metal layers with the formation of a Ga-doped $Zn_{1-x}Co_xO$ continuous layer with a thickness close to the total thickness of the S0 multilayer (figure 1(a)).

Table 1. EDX data for the S0 and S1 samples.

Sample	Ga/Zn	Co/Zn	O/(Zn + Ga + Co)
S0	3.05	7.53	0.78
S1	3.06	7.54	0.83

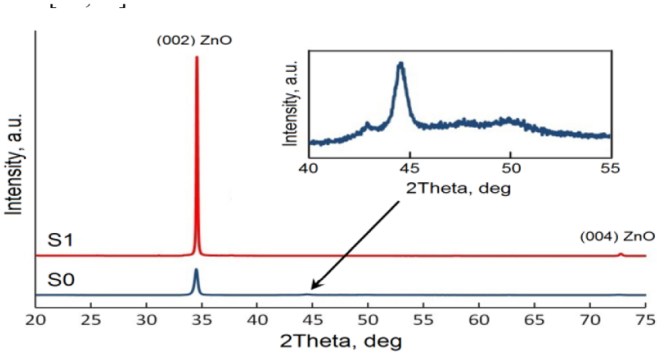

Figure 3. XRD patterns of the as-deposited (S0) and annealed (S1) samples. The inset shows the XRD spectral region with the Co-related peaks.

From the EDX analysis (table 1) the average Ga and Co content in the S0 and S1 samples was determined to be about 3 and 7.5 at. %, respectively. At the same time, as a result of annealing in air, the ratio O/(Zn + Co + Ga) grew from 0.78 to 0.83, which qualitatively indicates the oxidation of cobalt and the equalization of stoichiometry in ZnO.

An additional confirmation of the dissolution of cobalt in the ZnO crystal lattice is that the electrical conductance of the sample as a result of annealing, which initially consists of high conducting metal and GZO layers [24, 31], decreases by many orders of magnitude and becomes less than 10^{-6} S. This is consistent with literature results and is caused by the increased defect scattering due to the addition of Co^{2+} ions and the decrease in the n-type donor carrier concentration in Ga-doped $Zn_{1-x}Co_xO$ due to the trapping of free electrons from the intrinsic and extrinsic donor levels by the divalent Co ions [14, 34].

The XRD patterns of S0 and S1 samples are shown in figure 3. Only a single ZnO wurtzite phase with (002) preferential orientation is observed, suggesting that both samples retain the same crystalline structure and high c-axis orientation, which is typical for single-doped and undoped ZnO films, and for ZnO interlayers in the composition of multilayer structures [21, 24]. Additionally the XRD pattern of S0 features broad peaks related to the Co metal thin interlayers (inset of figure 3). After annealing these peaks disappear from the XRD spectrum, and the peaks related to any secondary phase (spinel and oxides) are not detected.

A comparison of the distinctive features of the (002) ZnO peak in the XRD spectra of the S0 and S1 samples is given in table 2. The S1 sample shows high intensity I and smaller integral width β for the (002) peak as compared to S0, indicating an improved crystallinity of the ZnO phase after high-temperature air annealing. The average crystallite sizes (CS) of ZnO calculated from the Scherrer formula ($CS = 0.9\lambda/(\beta\cos\theta)$, where λ is the wavelength of CuKα

Table 2. XRD data for ZnO phase in the S0 and S1 samples.

Sample	$2\theta_{002}$, deg	β_{002}, deg	I_{002}, cps	c, nm	CS, nm
S0	34.49	0.424	44 500	0.5200	26
S1	34.58	0.277	325 500	0.5184	63

x-rays, β is the peak integral breadth with no instrumental contribution, and θ is the peak Bragg angle) are 26 and 63 nm for S0 and S1, respectively. The observed shifts of the (002) peak with annealing indicate a reduction in the lattice constant ***c*** with Co doping, which is expected as slightly smaller Co ions are incorporated into the Zn sites of the ZnO lattice without changing the wurtzite structure [22]. Thus, the XRD data are in agreement with the optical properties and confirm the conclusion that there is a structural transformation: GZO/Co multilayer → Ga-doped $Zn_{1-x}Co_xO$ layer, as a result of annealing.

The magnetization (M) versus the applied magnetic field (H) using in-plane (ip) and out-of-plane (oop) configurations of VSM at room temperature for both the as-deposited (S0) and the annealed (S1) samples is plotted in figure 4.

In the case of the S0 sample, ferromagnetic behavior was observed for both configurations (figure 4(a)). The shape of the ip-magnetic hysteresis loops shows narrow loop characteristics in H, featuring a relatively low coercivity (~50 Oe) and high permeability, which reveal the typical character of soft magnetic materials. The single Co layer thickness also has to be considered, as its magnetic response changes, transitioning from a harder response below 5 nm, to a softer one above 20 nm [35]. It is obvious that the Co interlayers have a main ferromagnetic contribution to the total magnetization of the S0 multilayer, since undoped and Ga-doped ZnO films usually show a diamagnetic nature [30]. The lower coercivity is evidence of the partial amorphization of the thin Co interlayers [36].

Comparison among the up- and coop-hysteresis loops of the S0 sample shows that the easy magnetization axis was aligned in the film plane. In the pop-configuration the S0 saturation was not reached even at 15 kOe. In ZnO/Co multilayer systems the interfacial Co is composed of metallic Co, CoO_x ($x < 1$) and CoO [37]. The oxygen ions (O^{2-}) at the Co/ZnO interfaces can significantly affect the orbital attribute of the ferromagnetic Co by Co–O orbital hybridization and thereby mainly negatively affect the oop-magnetisation [37, 38].

It should be noted that the ip-hysteresis loop has a stepwise increase of the coercive field of the ferromagnetic interlayers (exchange-spring behavior [39]) (figure 4(b)). This loop form may be due to the presence of the crystalline cobalt phase and the amorphous cobalt phase with hard and soft magnetic properties, respectively, in the ferromagnetic interlayers of the sample [36]. It may also be caused by sequential magnetization reversal of three Co nanolayers [12]—for example, in the first stage, the magnetization reversal of the central Co interlayer occurs, since the demagnetizing fields of the outer layers are added to the external field. Then the external layers are magnetized too, along with an increase of the external field.

Field dependences of the magnetic moment of the sample after annealing of ZnO–Co indicate the absence of

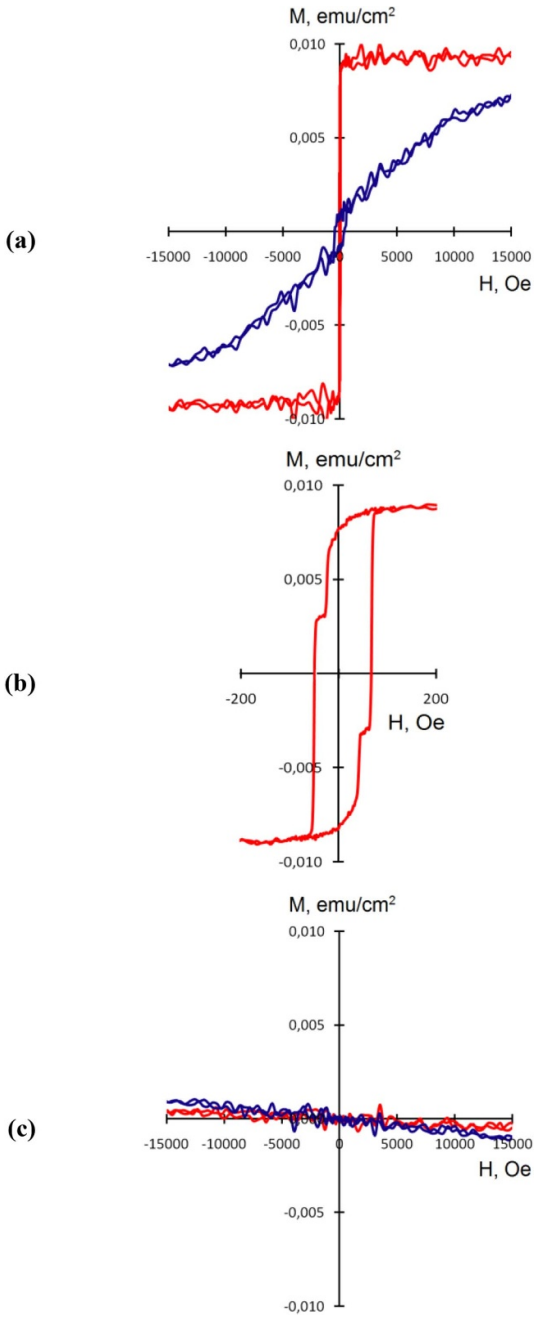

Figure 4. M–H plots of as-deposited (a), (b) and annealed (c) samples. Red line—ip configuration, blue line—oop configuration.

ferromagnetic ordering (figure 4(c)). The diamagnetic behavior of the S1 sample is observed in both measurement configurations, which can be interpreted as the diamagnetism of the quartz substrate and the absence or extremely small para- or ferromagnetic contribution from the Ga-doped $Zn_{1-x}Co_xO$ film. It should be noted that there is conflicting information about the magnetic properties of $Zn_{1-x}Co_xO$ solid solution systems at room temperature—many different types of behavior have been reported with TM-doped ZnO, such as being nonmagnetic, paramagnetic, ferromagnetic and antiferromagnetic depending on the method of sample preparation, variety of TM and doping level. The origin of RTFM in ZnO-based

DMS remains controversial. Different origins of RTFM, for example transition metal phase [37], secondary phase clusters [14, 36], an interfacial magnetic semiconductor [40] and the typical oxygen deficiency [26, 28] have been reviewed and proposed. Further, to explainthe intrinsic RTFM behavior of ZnO-based DMS various models were proposed, based on the exchange mechanism between electrons in the impurity atom and Zn lattice, the basis of bound magnetic polarons, the double exchange model in oxides and the Ruderman–Kittel–Kasuya–Yosida interaction.

Based on a review of various sources, we believe that the absence of ferromagnetism in the sample S1 is due to the fact that annealing was carried out in air at a sufficiently high temperature. The Curie temperature T_C for the $Zn_xCo_{1-x}O$ system is about 475 °C [41] and treatments of the sample at temperatures above T_C resulted in a rapid decrease in the ferromagnetic behavior or its total disappearance [41, 42]. According to our XRD data, for the GZO/Co multilayer annealed in air at 800 °C, only the ZnO phase with no metallic cobalt, CoO or $ZnCo_2O_4$ phases could be identified. In addition, the air annealing should lead to a decrease of oxygen vacancies in the Ga-doped $Zn_xCo_{1-x}O$. Therefore, the disappearance of both the ferromagnetic phase and oxygen vacancies, which play important roles in the RTFM of ZnO-based materials, resulted in the suppression of ferromagnetic behavior in the air-annealed sample.

Thus, from the point of view of utility of the obtained results for their potential application in spintronic and photonic devices, a further tuning of optical and magnetic properties of GZO/Co multilayers through optimization deposition and treatment processes is fundamental.

4. Conclusions

A GZO/Co seven-layer structure on quartz was consistently prepared by magnetron sputtering at a substrate temperature of 250 °C. The XRD patterns of the as-deposited multilayer revealed that the multilayer contains a nanocrystalline ZnO wurtzite phase with (002) preferential orientation and poor crystalline Co metal. The metal phase localized in thin continuous interlayers provided effective optical interference phenomena in the multilayer and its RTFM behavior. The shape of the hysteresis loop of the as-deposited sample, characterized by the narrowness and presence of steps, indicates typical soft magnetic properties of the pure crystalline Co interlayers and their stepped magnetization. As a result of annealing in air at 800 °C, the as-deposited diphase layered structure transforms into a monophase single layer of (002)-oriented Ga-doped $Zn_{1-x}Co_xO$ with x of about 11% due to the interdiffusion and cobalt dissolution without destroying the wurtzite structure ZnO. However, ferromagnetism was not detected in the annealed sample. Apparently it was due to the fact that the annealing completely suppressed the possibility of formation of ferromagnetic Co clusters and precipitates and also reduced the concentration of oxygen vacancies in the layer.

Acknowledgments

This research was performed in the frame of state assignments of the Ministry of Science and Higher Education of the Russian Federation for the Federal Scientific Research Center (FSRC) 'Crystallography and Photonics' of the Russian Academy of Sciences (RAS) and Dagestan Federal Research Center of RAS, and partially funded by the Russian Foundation for Basic Research (research project no. 18-29-12099). Access to the equipment of the Shared Research Center of FSRC 'Crystallography and Photonics' RAS was supported by the Ministry of Science and Higher Education of the Russian Federation (project RFMEFI62119X0035).

ORCID iDs

A Sh Asvarov https://orcid.org/0000-0001-6426-5006
A E Muslimov https://orcid.org/0000-0002-0524-7606
A Chiolerio https://orcid.org/0000-0001-9328-2999

References

[1] Benramache S, Benhaoua B and Bentrah H 2013 *J. Nanostruct. Chem.* **3** 54
[2] Cheng S, Ru Q, Liu P, Yan H, Shi Z, Hou X, Su S, Zhao L and Ling F-C-C 2019 *J. Alloy Compd.* **809** 151703
[3] Bairy R, Shankaragouda Patil P, Maidur S R, Vijeth V, Murari M S and Udaya B K 2019 *RSC Adv.* **9** 22302
[4] Shehata A, Tawfik W Z and Mohamed T 2020 *J. Opt. Soc. Am. B* **37** A1
[5] D'Agostino D, Di Giorgio C, Di Trolio A, Guarino A, Cucolo A M, Vecchione A and Bobba F 2017 *AIP Adv.* **7** 055010
[6] Bashir M I, Ali K, Sarfraz A K and Mirza I M 2016 *J. Alloy Compd.* **684** 151
[7] Shabannia R 2018 *Mater. Lett.* **214** 254
[8] Mani G K and Rayappan J B B 2015 *Mat. Sci. Eng. B* **191** 41
[9] Ali A, Henda R and Fagerberg R 2017 *Appl. Surf. Sci.* **422** 1082
[10] Poongodi G, Anandan P, Kumar R M and Jayavel R 2015 *Spectrochim. Acta A* **148** 237
[11] Atif M *et al* 2020 *J. Mater. Sci: Mater. Electron.* **31** 5253
[12] Schlage K, Bocklage L, Erb D, Comfort J, Wille H-C and Röhlsberger R 2016 *Adv. Funct. Mater.* **26** 7423
[13] Liu Y, Yang S, Wei G, Pan J, Yuan Y and Cheng C 2013 *J. Mater. Sci. Technol.* **29** 1134
[14] Bellingeri E, Rusponi S, Lehnert A, Brune H, Nolting F, Leveratto A, Plaza A and Marré D 2019 *Sci. Rep.* **9** 149
[15] Ying M, Blythe H J, Dizayee W, Heald S M, Gerriu F M, Fox A M and Gehring G A 2016 *Appl. Phys. Lett.* **109** 072403
[16] Neogi S K, Ahmed M A, Banerjee A and Bandyopadhyay S 2019 *Appl. Surf. Sci.* **481** 443
[17] Du F, Li Y, Li X, Yang J, Bai Y, Quan Z, Liu C and Xu X 2019 *J. Magn. Magn. Mater.* **489** 165445
[18] Kytin V G, Maximova O V, Kulbachinskii V A, Burova L I, Kaul A R, Bandyopadhya S, Ahmed A and Banerjee A 2018 *EPJ Web Conf.* **185** 06009
[19] Laurenti M *et al* 2017 *Sci. Rep.* **7** 41957
[20] Liu Y, Ding N, Gu G-R and Wu B-J 2019 *Ferroelectrics* **546** 120
[21] Abduev A K, Akhmedov A K, Asvarov A S, Muslimov A E and Kanevsky V M 2020 *Crystallogr. Rep.* **65** 491

[22] Henne B *et al* 2015 *Sci. Rep.* **5** 16863
[23] Chen S-F, Liu C-P, Hsu H S and Huang J C A 2008 *J. Appl. Phys.* **104** 083507
[24] Akhmedov A K, Abduev A K, Kanevsky V M, Muslimov A E and Asvarov A S 2020 *Coatings* **10** 269
[25] Kang S-G, Kim Y, Kim S E and Kim S 2013 *Electron. Mater. Lett.* **9** 7
[26] Kapilashrami M, Xu J, Ström V, Rao K V and Belova L 2009 *Appl. Phys. Lett.* **95** 033104
[27] Su X, Wang L, Chen J, Wan X, Zhang X and Wang R P 2011 *J. Phys. D: Appl. Phys.* **44** 265002
[28] Chithira P R and John T T 2020 *J. Magn. Magn. Mater.* **496** 165928
[29] Zhu L, Ye Z, Wang X, Ye Z and Zhao B 2010 *Thin Solid Films* **518** 1879
[30] Šutka A, Käämbre T, Joost U, Kooser K, Kook M, Duarte R F, Kisand V, Maiorov M, Döbelin N and Smits K 2018 *J. Alloy Compd.* **763** 164
[31] Abduev A, Akmedov A, Asvarov A and Chiolerio A 2015 *Plasma Process. Polym.* **12** 725
[32] Monks J N, Yue L, Yan B, Aldred B, Hurst A and Wang Z 2018 *Opt. Commun.* **429** 53
[33] Nenno D M *et al* 2019 *Sci. Rep.* **9** 13348
[34] Godavarti U, Mote V D and Dasari M 2017 *J. Asian Ceram Soc.* **5** 391
[35] Tiberto P, Gupta S, Bianco S, Celegato F, Martino P, Chiolerio A, Tagliaferro A and Allia P 2011 *J. Nanopart. Res.* **13** 245
[36] Wang Z, Zhao H, Yao Q, Xu J and Kimura H 2013 *J. Magn. Magn. Mater.* **345** 41
[37] Meng F, Feng C, Wang L, Li Y, Yao M, Xu X, Li B, Hu Q, Hu L and Yu G 2020 *Appl. Phys. Lett.* **116** 022414
[38] Gweon H K, Yun S J and Lim S H 2018 *Sci. Rep.* **8** 1266
[39] Quan Z, Zhang X, Liu W, Li X, Addison K, Gehring G A and Xu X 2013 *ACS Appl. Mater. Interfaces* **5** 3607
[40] Magnus F *et al* 2016 *Nat. Commun.* **7** 11931
[41] Song C, Zeng F, Geng K W, Wang X B, Shen Y X and Pan F 2007 *J. Magn. Magn. Mater.* **309** 25
[42] Prellier W, Fouchet A, Mercey B, Simon C and Raveau B 2003 *Appl. Phys. Lett.* **82** 3490